

# Shake Table Tests on Infill Plasterboard Partitions

Gennaro Magliulo<sup>\*a</sup>, Crescenzo Petrone<sup>a</sup>, Vittorio Capozzi<sup>a</sup>, Giuseppe Maddaloni<sup>b</sup>, Pauline Lopez<sup>c</sup>, Renato Talamonti<sup>d</sup> and Gaetano Manfredi<sup>a</sup>

<sup>a</sup>University of Naples Federico II, Department of Structural Engineering, via Claudio 21, 80125 Naples, Italy. <sup>b</sup>University of Naples Parthenope, Department of Technology, Centro Direzionale, Isola C4, 80143 Naples, Italy; <sup>c</sup>Etex Dry Co, Product Development Department, 500 Rue Marcel Demonque, 84915 Avignon, France; <sup>d</sup>Lafarge Gessi, via G. G. Winckelmann 2, 20146 Milan, Italy

**Abstract:** Shaking table tests are performed to investigate the seismic behaviour of plasterboard partitions. A steel test frame is properly designed in order to simulate the seismic effects at a generic building storey. The tests are performed shaking the table simultaneously in both horizontal directions. At this aim the accelerograms are selected matching the target response spectrum provided by the U.S. code for nonstructural components. To investigate a wide range of interstorey drift demand and seismic damage, the shakes are performed scaling the accelerograms at eight different intensity levels. The tested plasterboard partitions exhibit a good seismic behaviour, both in their own plane and out-of-plane, showing light damage up to 0.8% interstorey drift ratio and 2g top frame acceleration.

Finally, an interesting comparison of the dynamic characteristics, i.e. fundamental period and damping ratio, between the bare frame and the infilled structure is also performed using different methods.

**Keywords:** Dynamic identification, Infilled frame, Infill plasterboard partitions, Nonstructural components, Seismic performance, Shaking table test.

## INTRODUCTION

As widely known, nonstructural components are a very critical issue in earthquake seismic zones. The damages on nonstructural components cause the largest part of the economic loss [1], besides causing evacuation of buildings and their use interruption [2].

Nevertheless few experimental studies on plasterboard partitions are available in literature. The behaviour of partitions and suspended ceilings during earthquakes is discussed in [3]. Full-scale drywall partitions with light-gage steel stud framing were tested to observe damage in cyclic loading conditions in [4]. In [5] a shake table test on a full-scale 4 story steel building, in which various non-structural components were installed (i.e. both plasterboard partitions and suspended ceilings) to evaluate their seismic performance, is presented.

Moreover, infill walls in frame structures are widely recognized to affect both the strength and stiffness of infilled-frame structures [6-9]. In particular, the infill walls can significantly increase the lateral stiffness, causing a very different seismic demand with respect to the prediction by the analyses on bare structural model.

In this paper the influence of innovative plasterboard partitions on a steel frame structure is investigated. Such partitions are designed in order to not interfere with the hosting structure up to moderate level of drifts (~0.5%).

## Experimental Facilities and Test Set Up, Specimens and Input

The seismic qualification of infill plasterboard partitions is carried out by the earthquake simulator system available at the laboratory of Structural Engineering Department of University of Naples Federico II. The system consists of two 3m x 3m square shake tables. Each table is characterized by two degrees of freedom in the two horizontal directions. Only one shake table is used in this experimental campaign.

The tests aim to investigate the seismic behaviour of particular drywall partitions made by the Lafarge Plâtres industry. Lafarge is a company present in 78 countries and world leader in building materials.

With the purpose of simulating the seismic effects on the partition, a steel test frame is properly designed according to Eurocodes [10-12] and built (Fig. 1). The geometry of the test frame is defined taking into account two requirements: (a) realistic value of mass; (b) lateral stiffness resulting in interstorey displacement  $d_r = 0.005 h$  (being  $h$  the interstorey height) for a 50 years return period earthquake typical of a high seismicity zone.

The result is a 2.50 m (X dir.) x 2.00 m (Y dir.) x 2.89 m (Z dir.) inverted pendulum test fixture. The test frame is composed of welded square hollow columns (150 mm x 150 mm x 15 mm) of C45 steel material and rolled square hollow beams (120 mm x 120 mm x 12.5 mm) of steel S275; the beam-column connections are bolted. A reinforced concrete slab of class C45/55 is placed on the roof of the structure (Fig. 1).

\*Address correspondence to this author at the University of Naples Federico II, Department of Structural Engineering (DIST), via Claudio, 21, I-80125 Naples, Italy; Tel: +39 081 768 3656; Fax: +39 081 768 5921; E-mail: [gmagliul@unina.it](mailto:gmagliul@unina.it)

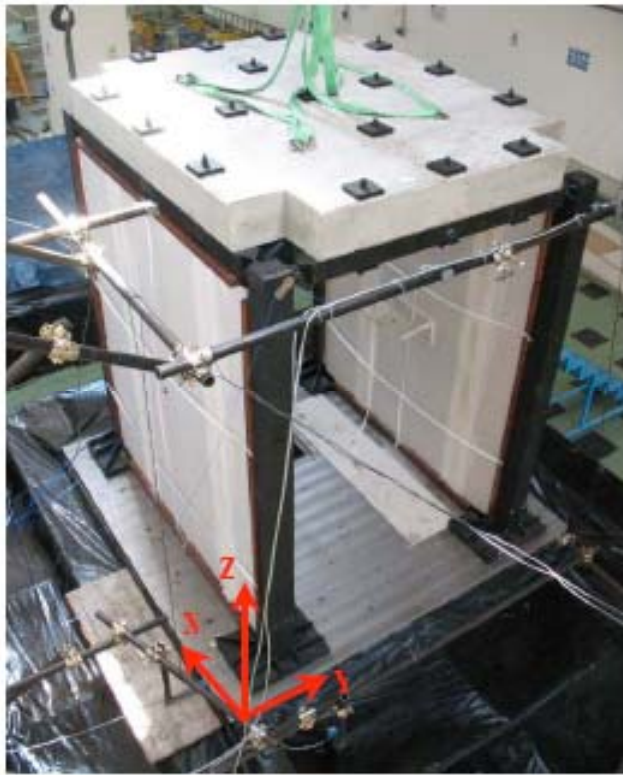


Fig. (1). Scheme of test setup: overview.

Wooden beams are also placed along the perimeter of two longitudinal bays, having a technological purpose: they allow the installation of the plasterboard partition guides.

Two partitions are contemporary tested in order to maintain symmetry in the seismic behaviour of the test frame.

A schematic representation of the test specimen is shown in Fig. (2). The main components are: the “base and lateral runners”, U-steel section profiles screwed respectively to base floor and columns, with dimension 40-75-40 mm, 6/10 mm thick; the “top runner”, an U-steel section profile

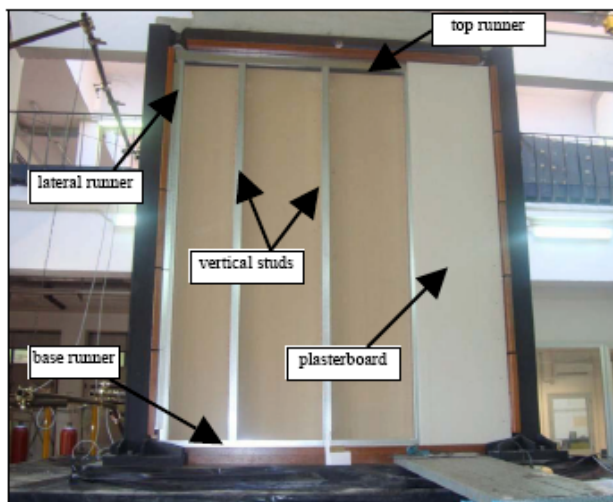


Fig. (2). Infill plasterboard partition: overview.

screwed to top floor, with dimension 80-75-80 mm, 10/10 mm thick; “vertical studs”, U-section profiles housed in the upper and lower runners, but not screwed to them, with dimension 47-74-50 mm, 6/10 mm thick, spaced 600 mm. Two layers compose the drywall partitions: the so-called “PREGYPLAC BA13 plasterboards” and “PREGY LaDURA BA13 plasterboards”, weighing 90 N/m<sup>2</sup> and 128 N/m<sup>2</sup> respectively (Fig. 3). The latter is a plasterboard with high mechanical resistance conferred by wood fibres. Each layer, according to EN 520 [13], is 12,5 mm thick and with thinned edges. The plasterboards are screwed only on vertical studs. The gap, properly defined between the plasterboards and the perimeter, is filled with acrylic silicone. Such system is designed in order not to interfere with the relative displacement of the housing structure up to 0.5% drift.

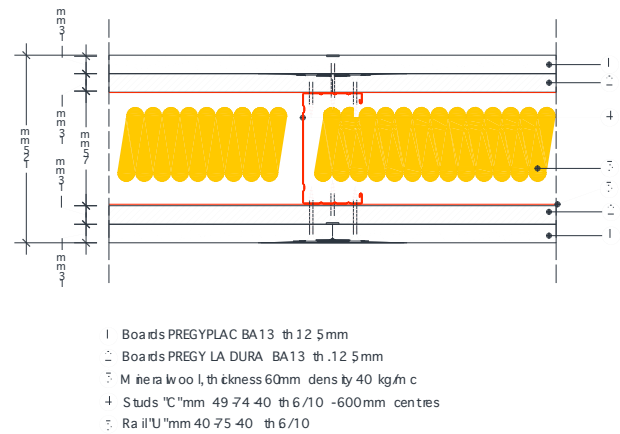


Fig. (3). Cross section of the double layer of drywall partition.

Six accelerometers and six laser-optical sensors are used to monitor the response of the test frame and partitions.

The input to the table is provided through acceleration time histories representative of expected/target ground motion and acting simultaneously along the two horizontal directions; the time histories are artificially defined in order to match the required response spectrum (RRS), provided by the ICBO-AC156 code “Acceptance criteria for seismic qualification testing of nonstructural components” [14].

According to ICBO, the RRS is obtained as a function of the spectral acceleration called  $S_{DS}$ .  $S_{DS}$  is the parameter that characterizes the ground motion. For horizontal design-basis earthquake shaking, the International Building Code [15] defines the short period design basis earthquake acceleration response as:

$$S_{DS} = \frac{2}{3} \cdot F_A \cdot S_S$$

where  $F_A$  is a site soil coefficient, set equal to 1 in this study, and  $S_S$  is the mapped maximum considered earthquake (MCE) spectral acceleration at short periods.

The selected procedure is performed for a Required Response Spectrum corresponding to a given  $S_{DS}$ . The records are then scaled to match the other levels of the target spectrum, defined later.

The matching procedure is ensured over the frequency range from 1.3 to 33.3 Hz; the elastic response spectrum ordinates shall not be lower than 0.9 times RRS and larger than 1.3 times RRS. Two different time histories are defined for the two horizontal directions.

Fig. (4). shows the obtained acceleration time histories for the X and Y directions in terms of acceleration, velocity and displacement, their elastic response acceleration spectra, the RRS corresponding to  $S_{DS}$  equal to 0.30g and the RRS scaled to 90% and 130%.

More details concerning the procedure to select the accelerograms used as drive motions for the tests are described [16].

Eight bidirectional tests with different intensity values, ranging from  $S_{DS} = 0.10g$  to  $S_{DS} = 1.05g$ , are performed (Table 1).

**Dynamic Identification**

Different procedures are used to evaluate the fundamental period and the damping ratio of the test setup. In order to evaluate the influence of the plasterboard partitions, the procedure is applied both on the bare steel frame and on the infilled structure. It should be noted that the main objective of this test campaign is related to the evaluation of the seismic performance of the plasterboard partitions; for this reason, the study is mostly related to the dynamic behaviour of the infilled frame.

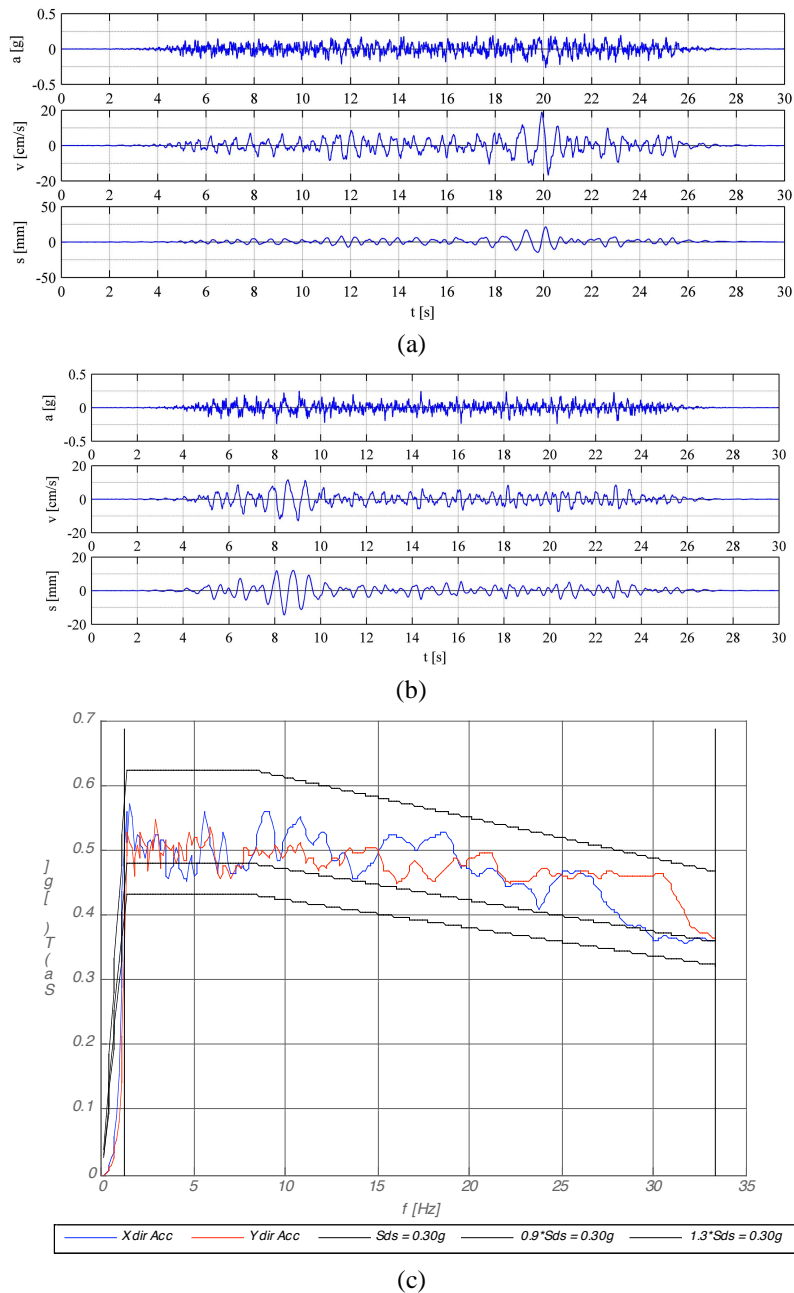


**Fig. (4).** Earthquake time histories and spectra for  $S_{DS}$  equal to 0.30g: (a) acceleration, velocity and displacement time-history - X direction; (b) acceleration, velocity and displacement time-history - Y direction; (c) input accelerogram spectra, RRS (bold line), upper and lower limits (dashed line), matching frequency range.

**Table 1.  $S_{DS}$  Values for 8 Input Test Levels**

Test No.	$S_{DS}$ x direction	$S_{DS}$ y direction
[-]	[g]	[g]
1	0.10	0.10
2	0.15	0.15
3	0.22	0.22
4	0.30	0.30
5	0.45	0.30
6	0.60	0.30
7	0.90	0.30
8	1.05	0.30

Three methods are illustrated in the following. For each method, the results concerning the bare steel test frame are presented; the method no. 1 is also applied on the infilled frame.

**Method 1**

This method consists of applying to the base of the test frame a harmonic drive motion with predefined amplitudes and frequency  $f$ . The maximum acceleration on the roof of the bare test frame  $\ddot{u}_{max,top}$  and the harmonic base amplitude  $\ddot{u}_{max,base}$  are recorded for each frequency  $f$ . The transmissibility ratios  $TR = \frac{\ddot{u}_{max,top}}{\ddot{u}_{max,base}}$  are then evaluated (blue dots in

Fig. 5). The peak of the curve gives the natural frequency  $f_n$ , while the damping ratio is evaluated applying the half-bandwidth method.

The procedure points out a fundamental frequency  $f_n$  of 3.81Hz and a 0.92% damping ratio.

In Fig. (5) the experimental points are also fitted with the theoretical curve (pink line), using the following relationship [16]:

$$TR = \left\{ \frac{1 + [2 \cdot \xi \cdot (f/f_n)]^2}{[1 - (f/f_n)^2]^2 + [2 \cdot \xi \cdot (f/f_n)]^2} \right\}^{1/2}$$

As shown in the figure, the very low damping generates a very high amplification close to the resonance frequency, causing very high accelerations and inertial forces on the test frame roof; in order to avoid the test frame going into the inelastic range, limited points are evaluated in this region.

Note that the half-bandwidth method is theoretically valid for a displacement response factor  $R_d$  - frequency curve [17]. Nevertheless, this method is applicable still in the case of TR - frequency curve since they are very close one an-

other around the peak [17]. Indeed, the ratio  $TR/R_d$  is theoretically evaluated as.

$$\frac{TR}{R_d} = \sqrt{1 + (2 \cdot \xi \cdot f/f_n)^2}$$

resulting in ratio very close to 1 for the typical values of damping and for frequency not so far from the resonance (see Fig. 6).

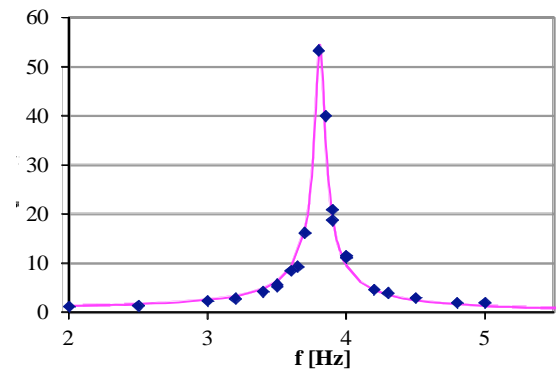


**Fig. (5).** Transmissibility ratios curve for the bare steel frame.

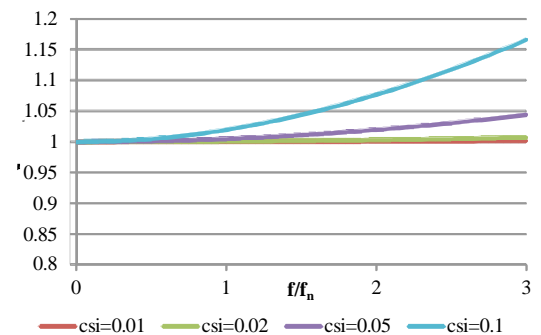


**Fig. (6).** Ratio between theoretical Transmissibility ratio TR and Displacement response factor  $R_d$  for different damping values (csi).

As clearly shown in Fig. (6), the value of TR for  $f=f_n$  is very close to the value of  $R_d$ . This implies that the damping ratio can be also evaluated as:

$$\zeta = \frac{1}{2 \cdot R_{d,f=f_n}} \cong \frac{1}{2 \cdot TR_{f=f_n}}$$

The formula yields a 0.94% damping ratio. However, this value can be considered an upper bound of the damping ratio, due to the lack of experimental points close to the resonance, as highlighted above.

The procedure is also applied on the infilled frame in order to evaluate the influence of the partitions on the dynamic parameters of the test setup. A 8.33% damping value is evaluated upon the transmissibility curve peak Fig. (7). the peak occurs at 4.02Hz, defining a very light increase of the natural frequency and a significant influence of the partitions on the damping ratio. The half bandwidth method, instead, gives out a 5.42% damping ratio.

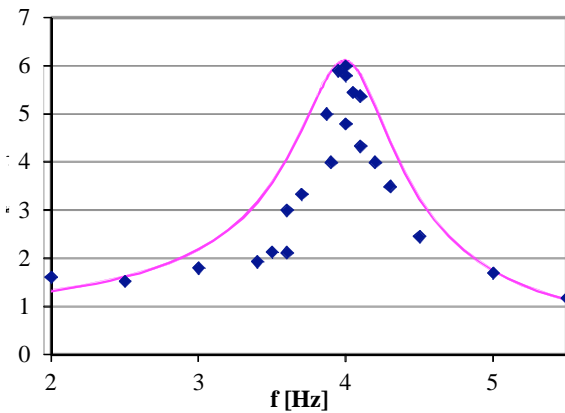


Fig. (7). Transmissibility ratios curve for the infilled structure.

**Method 2**

The transfer curve method is also used to evaluate the natural frequency and the damping ratio of the bare test frame. The transfer function is defined, in this case, as the ratio of the roof acceleration response to the input base motion, i.e. a white noise time history, in the frequency domain [18].

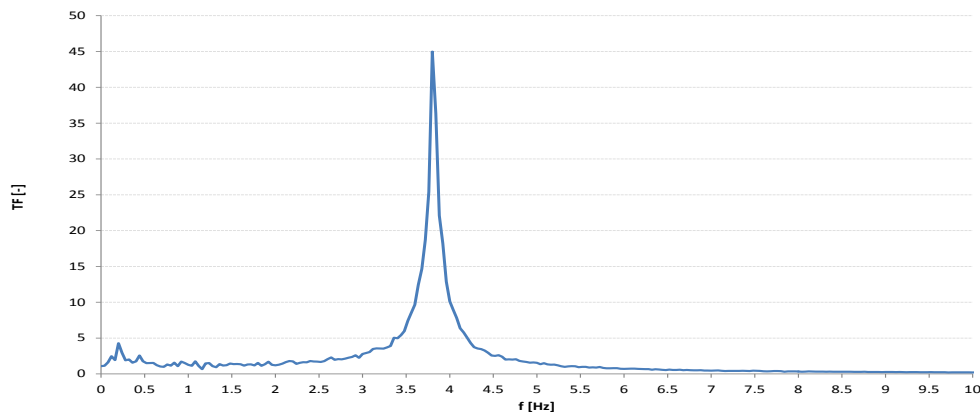


Fig. (8). Transfer function generated by a white noise input on the bare structure.

The half-bandwidth method is used for the damping ratio evaluation, while the peak denotes the natural frequency of the system.

A 3.86Hz natural frequency and 1.5% damping ratio are evaluated for a white noise input motion Fig. (8).

**Method 3: Free Vibration Decay**

This method allows the evaluation of the damping ratio value in free vibration conditions upon the ratio of two peak displacements measured over m consecutive cycles [19].

$$\zeta = \frac{1}{2 \cdot \pi \cdot m} \ln \frac{u_i}{u_{i+m}}$$

In case of lightly damped systems this procedure can be adopted in term of accelerations that usually are easily recorded:

$$\zeta = \frac{1}{2 \cdot \pi \cdot m} \ln \frac{\ddot{u}_i}{\ddot{u}_{i+m}}$$

This procedure is applied referring to the acceleration time history recorded after a shaking quite intense ( $\ddot{u}_{roof} > 1.5g$ ). Due to the very low level of damping recorded, the test frame continues vibrating significantly for many cycles (black box in Fig. (9)).

In order to apply such procedure, the signal was band-pass filtered in a frequency range close to the natural frequency, obtaining the red curve in Fig. (9).

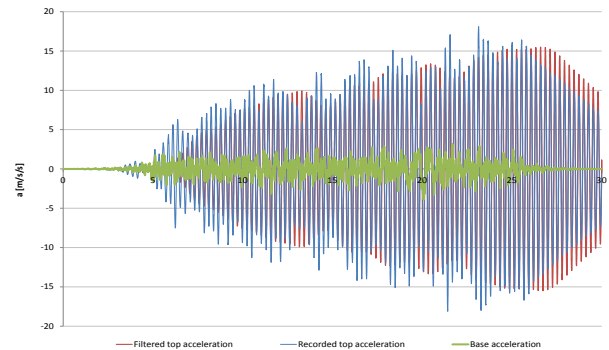


Fig. (9). Acceleration time history recorded at the base of the test frame, Filtered and recorded acceleration time histories at the top of the test frame. The black box indicates the region in which the free vibration decay method is applied.

**Table 2. Damping Evaluation According to Free Vibration Decay Method – Positive Cycles**

$\zeta$ [%]		$i+m^{\text{th}}$ cycle											
		2	3	4	5	6	7	8	9	10	11	12	13
$i^{\text{th}}$ cycle	1	0.05	0.13	0.22	0.30	0.37	0.42	0.47	0.50	0.53	0.56	0.58	0.60
	2		0.21	0.30	0.38	0.45	0.50	0.54	0.57	0.59	0.62	0.64	0.66
	3			0.39	0.46	0.52	0.57	0.61	0.63	0.65	0.67	0.68	0.70
	4				0.53	0.59	0.63	0.66	0.68	0.69	0.71	0.72	0.73
	5					0.65	0.68	0.70	0.71	0.72	0.73	0.75	0.76
	6						0.71	0.73	0.74	0.74	0.75	0.76	0.77
	7							0.74	0.75	0.75	0.76	0.77	0.78
	8								0.75	0.76	0.77	0.78	0.79
	9									0.76	0.78	0.79	0.80
	10										0.79	0.80	0.82
	11											0.82	0.83
	12												0.84

**Table 3. Damping Evaluation According to Free Vibration Decay Method – Negative Cycles**

$\zeta$ [%]		$i+m^{\text{th}}$ cycle											
		2	3	4	5	6	7	8	9	10	11	12	13
$i^{\text{th}}$ cycle	1	0.12	0.21	0.30	0.37	0.43	0.48	0.52	0.55	0.58	0.60	0.62	0.64
	2		0.30	0.38	0.46	0.51	0.56	0.59	0.61	0.63	0.65	0.67	0.69
	3			0.46	0.53	0.58	0.62	0.64	0.66	0.68	0.69	0.71	0.73
	4				0.60	0.64	0.67	0.69	0.70	0.72	0.73	0.74	0.75
	5					0.68	0.70	0.72	0.73	0.74	0.75	0.76	0.77
	6						0.73	0.74	0.75	0.75	0.76	0.77	0.79
	7							0.75	0.75	0.76	0.77	0.78	0.80
	8								0.76	0.77	0.78	0.79	0.81
	9									0.78	0.79	0.80	0.82
	10										0.80	0.82	0.83
	11											0.84	0.85
	12												0.86

The procedure is applied with respect to all the possible peaks couple combinations. In Tables 2 and 3 the damping ratio is evaluated and listed referring to the peak decay from the  $i^{\text{th}}$  cycle (rows) to the  $i+m^{\text{th}}$  cycle (columns). Averaging the results, the damping ratio value is estimated to be  $\zeta = 0.649\% \pm 0.162\%$ .

The results of the dynamic identification procedures are summarized in the Table 4.

Upon these results, it can be concluded that:

- The innovative plasterboard partitions do not influence the natural frequency of the test frame. The goal of not interfering with the hosting structure is achieved;

- The damping ratio of the setup significantly increases with the insertion of the partition within the test frame, causing a beneficial effect in the dynamic response.

### Test Results and Comparison

Using the selected drive motions, eight bidirectional shaking tests are performed. The maximum recorded values of acceleration at the base and at the roof of the test frame are 1.03g and 2.22g respectively; the maximum accelerations of the partitions are 1.82g and 1.81g, in plane and out-of-plane respectively. As visible, due to dynamic amplification, the maximum value of acceleration recorded at the base of the table is completely different from the ones recorded on the roof and on the partitions. This aspect may be crucial for

experimental tests on shaking table. For this reason, the procedure described in [20], concerning the optimization of the drive motion to predict the signal recorded at desired locations, i.e. on the partitions, using a compensation procedure, will be taken into account in the next experimental campaigns.

Relative displacements are also evaluated using the laser sensors records. The maximum recorded relative displace-

- LSLS → Life safety limit state (damage state 3 limit).

After each test, damage is observed inspecting the specimen components. The recorded damage in each component is then correlated to one of the three limit states defined above. Indeed, in Table 5 the level of damage required to reach a limit state is defined for each damage typology of each system component (i.e. plasterboards, studs, runners

**Table 4. Summary of the Results Obtained with the Different Procedures**

<i>Method</i>	Transmissibility curve			Transfer curve		Free vibration decay
<i>Structure</i>	$f_n$ [Hz]	$\zeta_p$ [%]	$\zeta_{HB}$ [%]	$f_n$ [Hz]	$\zeta$ [%]	$\zeta$ [%]
<b>Bare frame</b>	3.81	0.94%	0.92%	3.86	1.55%	0.65%
<b>Infilled frame</b>	4.02	8.33%	5.42%	-	-	-

ments are 20.1mm in X direction and 22.7mm in Y direction. The maximum interstorey drifts are evaluated considering the column height, i.e. 2740 mm. Values up to 0.83% drift are recorded, representative of a moderate earthquake intensity level.

In this study three limit states are considered for the seismic response definition of the plasterboard partitions and in particular:

- OLS → Operational limit state (damage state 1 limit);
- DLS → Damage limit state (damage state 2 limit);

and screws). This damage is defined quantitatively, if possible; in the opposite case a qualitative definition of the level of damage is defined.

The shake table tests show a very slight damage (Fig. 10) including:

- Slight cracking in vertical joints between plasterboards;
- Acrylic silicone detachment (inserted in the separation between partition and wooden vertical support);
- Chalk dust fall.

Such level of damage was assessed unable to reach even

**Table 5. Damage State Definition Upon the Damage Recorded Within Each Component of the Partition System**

System Component	Damage typology	OLS (damage state 1 limit)	DLS (damage state 2 limit)	LSLS (damage state 3 limit)
		need for minor repairs	need to remove and replace the partition	human life hazard
Plasterboard	collapse / cracking	cracks that compromise partition use	cracks extended at least for partition half dimension / not repairable break (edges)	partition portion collapse (>0,75mq) with consequent dislocation
Plasterboard	overturning	\	\	partition overturning
Stud	collapse	small permanent deformations	track movement with respect to its initial position/ great deformations/ flange opening	track collapse (shear, bending, instability)
Runner on the floor	collapse	small permanent deformations	track movement with respect to its initial position/ great deformations/ flange opening	guide crisis (failure, total detaching of the connection)
Runner beneath the roof	collapse	small permanent deformations	track displacement with respect to its initial position/ great deformations/ flange opening	guide crisis (failure, total detaching of the connection)
Screws	fracture	release of small number of screws respect their initial position (at least 10%)	some screws loosening or breaking that causes partial separation of one or more components / breaking and/or release of at least 30% of screws	breaking of many screws that lead the partition to collapse or overturning / break of at least 50 % of screws

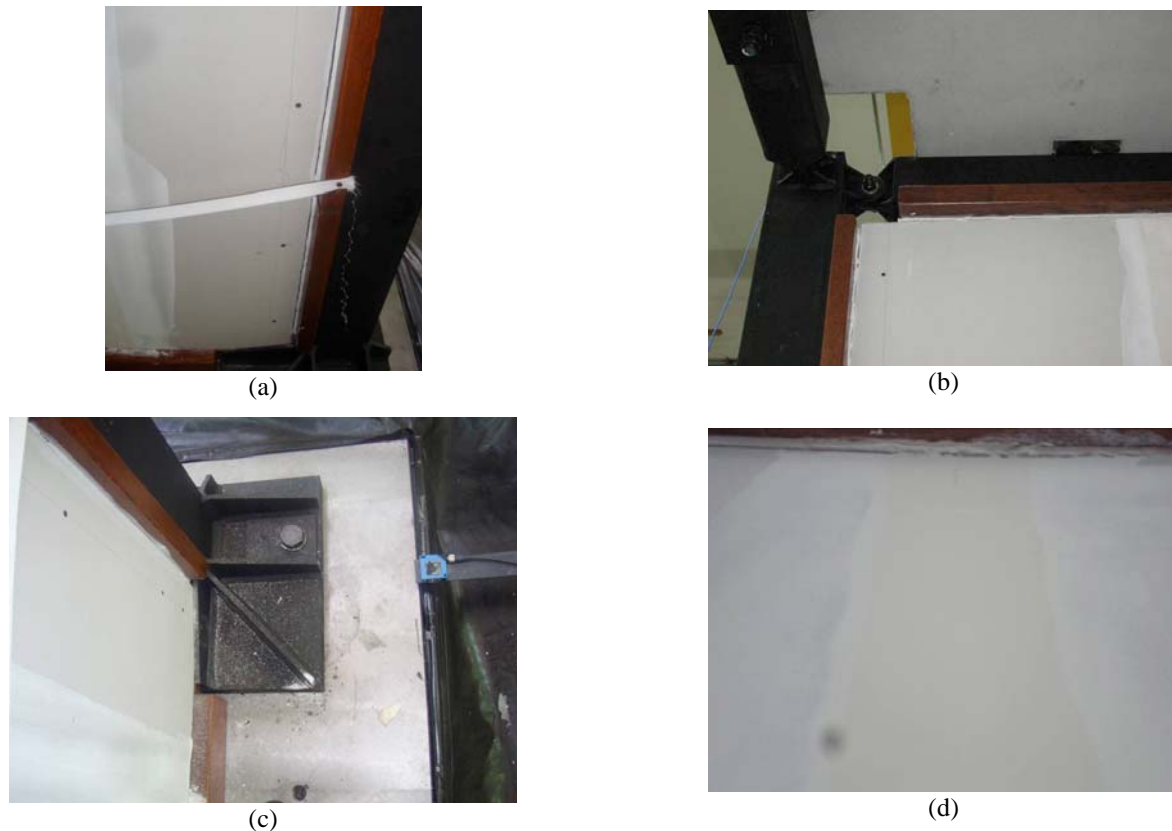


**Fig. (10).** Photos of the light damages recorded after the bidirectional shake table tests: (a) and (b) acrylic silicon detachment, (c) chalk dust fall, (d) light cracking in vertical plasterboard joints.

the limit state 1.

## CONCLUSIONS

In order to investigate the seismic behaviour of infill plasterboard partitions, shaking table tests are carried out by the earthquake simulator system available at the laboratory of Structural Engineering Department of University of Naples Federico II.

The tests aim to investigate the seismic behaviour of particular drywall partitions made by the Lafarge Plâtres industry and a steel test frame is properly designed and built to the purpose.

Using drive motions properly selected for the tests, eight bidirectional shakings are performed. The maximum recorded values of acceleration at the base and on the roof of the test frame are 1.03g and 2.22g respectively; the maximum accelerations on the partitions are 1.82g and 1.81g, in plane and out-of-plane respectively.

Test results show a very light damage also for an acceleration level equal to 2g (representative of 0.4g ground acceleration) and 0.8% interstorey drift.

The dynamic identification procedure and the experimental evidence show that the tested partitions do not contribute to the structural stiffness. Indeed, no variations in terms of stiffness and structural period are recorded after introducing the partitions within the test frame; moreover, the partitions

implies a damping increase, resulting in a beneficial effect in relation to the earthquake. For this reason, they can be catalogued as non-interacting partitions in the framework of the non-structural components defined in Eurocode 8. This allows the benefit of designing much more flexible and economic structures, satisfying the relationship  $d_r \cdot v \leq 0.010 \cdot h$ .

## CONFLICT OF INTEREST

The authors confirm that this article content has no conflicts of interest.

## ACKNOWLEDGEMENTS

This research study has been funded both by Italian Department of Civil Protection in the frame of the national project DPC - ReLUIS 2010-2013 and by Lafarge that also provided the components for the testing program.

The authors also acknowledge the collaboration of MS Engineer Francesco Martucciello in the design and execution of experimental tests.

## REFERENCES

- [1] S. Taghavi, and E. Miranda, "Response Assessment of Nonstructural Building Elements", PEER Report 2003/05, College of Engineering, University of California Berkeley, USA, 2003.
- [2] G. Magliulo, V. Pentangelo, and G. Manfredi, "Danneggiamento delle controsoffittature a seguito del terremoto dell'Aquila dell'aprile 2009" V1.00. Available on <http://www.reluis.it> (in Italian).

- [3] S. Rihal, and G. Granneman, "Experimental Investigation of the Dynamic Behavior of Building Partitions and Suspended Ceilings During Earthquakes", Rep. No. ARCE R84-1, California Polytechnic State University, Pomona, CA, USA, 1984.
- [4] T.-H. Lee, M. Kato, T. Matsumiya, K. Suita, and M. Nakashima, "Seismic performance evaluation of non-structural components: drywall partitions". *Earthquake Eng. Struct. Dyn.*, vol. 36, pp. 367-382, 2007.
- [5] Y. Matsuoka, K. Suita, S. Yamada, Y. Shimada, and M. Akazawa, "Non-structural component performance in 4-story frame tested to collapse", In: *Proceedings of the 14<sup>th</sup> World Conference on Earthquake Engineering*, October 12-17, 2008, Beijing: China 2008.
- [6] P.G. Asteris, "Lateral Stiffness of brick masonry infilled plane frames, *Struct. Eng., Am. Soc. of Civil Eng. (ASCE)*, vol. 129, no. 8, pp. 1071-1079, 2003.
- [7] P.G. Asteris, "Finite element micro-modeling of infilled frames", *Electron. J. Struct. Eng.*, vol. 8, pp. 1-11, 2008.
- [8] P.G. Asteris, D.J. Kakaletsis, C.Z. Chrysostomou, and E.E. Smyrou, "Failure modes of infilled frames", *Electron. J. Struct. Eng.*, vol. 11, no. 1, pp. 11-20, 2011.
- [9] G. Magliulo, V. Capozzi, R. Ramasco. "Seismic performance of R/C frames with overstrength discontinuities in elevation". *Bull. Earthquake Eng.*, vol. 10, no. 2, pp. 679-694, DOI: 10.1007/s10518-011-9316-9, 2012.
- [10] CEN, Eurocode 3: design of steel structures - Part 1-1: General rules and rules for buildings. EN 1993-1-1, Brussels, Belgium, 2005.
- [11] CEN, Eurocode 3: design of steel structures - Part 1-8: design of joints. EN 1993-1-8, Brussels, Belgium, 2005.
- [12] CEN, Eurocode 8: design of structures for earthquake resistance - Part 1: general rules, seismic actions and rules for buildings. EN 1998-1, Brussels, Belgium, 2004.
- [13] UNI, UNI-EN 520:2009, Plasterboards – Definitions, requirements and testing protocol, Milano, Italy, 2009 (in Italian).
- [14] International Conference of Building Officials (ICBO) ICBO AC 156, "Acceptance Criteria for the Seismic Qualification of Non-structural Components", ICBO Evaluation Service, Inc., Whittier, California, USA, 2000.
- [15] International Code Council (ICC), "International Building Code, 2000 Edition (IBC 2000)", Falls Church, Virginia, 2002.
- [16] G. Magliulo, and G. Manfredi, "Shaking Table Test For Analysis Of Seismic Performance Of Lafarge Plasterboard Partitions", Report no. 2010078-02, Department of Structural Engineering, University of Naples Federico II, Italy, 2011.
- [17] A.K. Chopra, *Dynamics of Structures*. Prentice Hall: Englewood Cliffs, New Jersey, 1995.
- [18] J.M. Bracci, A.M. Reinhorn, and J.B. Mander, "Seismic Resistance of Reinforced Concrete Frame Structures Designed Only for Gravity Loads: Part I – Design and Properties of a One-Third Scale Model Structure", Technical Report NCEER-92-0027, University of Buffalo, The State University of NY, December 1992.
- [19] R.W. Clough, and J. Penzien, *Dynamics of Structures*, 3<sup>rd</sup> ed. Computers & Structures, Inc: Berkeley 1995.
- [20] G. Maddaloni, K.P. Ryu and A.M. Reinhorn. "Simulation of floor response spectra in shake table experiments". *Earthquake Eng. Struct. Dyn.*, vol. 40, no. 6, pp. 591-604, DOI: 10.1002/eqe.1035, 2011.

---

Received: March 03, 2012

Revised: June 02, 2012

Accepted: June 04, 2012

© Magliulo *et al.*; Licensee Bentham Open.

This is an open access article licensed under the terms of the Creative Commons Attribution Non-Commercial License (<http://creativecommons.org/licenses/by-nc/3.0/>) which permits unrestricted, non-commercial use, distribution and reproduction in any medium, provided the work is properly cited.